Synthesis of two-dimensional titanium nitride Ti_4N_3 (MXene)

Patrick Urbankowski,[1]* Babak Anasori,[1]* Taron Makaryan,[1] Dequan Er,[2] Sankalp Kota,[1] Patrick Walsh,[1] Mengqiang Zhao,[1] Vivek B. Shenoy,[2] Michel W. Barsoum, [1] Yury Gogotsi[1†]

[1]A.J. Drexel Nanomaterials Institute and Department of Materials Science & Engineering, Drexel University, Philadelphia, PA 19104, USA
[2]Department of Materials Science and Engineering, University of Pennsylvania, Philadelphia, Pennsylvania 19104, USA

*Contributed equally to this work
[†]Corresponding author: Y. Gogotsi (gogotsi@drexel.edu) Tel.: +1-215-895-6446 Fax: +1-215-895-1934

I. Ti_4AlN_3 and $Ti_4N_3T_x$ synthesis

The precursor Ti_4AlN_3, MAX phase, was produced by mixing TiH_2 (TIMET, Henderson, NV; 99.3 % -325 mesh), AlN (Alfa Aesar, Ward Hill, MA; N 32.0 % minimum, 2.5 to 4.0 μm), and TiN (Alfa Aesar, Ward Hill, MA; 99.8 %, 2 to 5 μm) powders with a molar ratio of 2 : 1 : 2. These powders were ball milled for 14 h and hot pressed for 24 h at 1275 °C and 70 MPa.[1] The resulting Ti_4AlN_3 block was then milled using a drill bit and sieved through a 400 mesh, producing a powder with particles smaller than 37 μm. The fluoride salt was a mixture of potassium fluoride (KF), lithium fluoride (LiF) (98.5 %, -325 mesh), and sodium fluoride (NaF) (all Alfa Aesar, Ward Hill, MA) with a mass ratio of 0.59 : 0.29 : 0.12, respectively, chosen because this is the eutectic composition of these salts, which allows for this treatment to be performed at lower temperature.[2] The Ti_4AlN_3 was then mixed with the fluoride salt mixture in a 1 : 1 mass ratio and ball milled for 6 h. The mixture, a 2 g batch of Ti_4AlN_3 and fluoride salt, was then placed into an alumina crucible. Unlike in previous methods of heating MAX phases in molten salt in air,[3] this treatment was performed in Ar. The treatment was performed at 550 °C for 30 min, with heating and cooling rates of 10 °C/min.

After the molten salt treatment, XRD detected several fluorides including cryolite (Na_3AlF_6) and other similar Al-containing fluorides: K_2NaAlF_6, K_3AlF_6, AlF_3 and $LiNa_2AlF_6$. Diluted sulfuric acid (H_2SO_4) (Fisher Scientific, Fair Lawn, NJ; > 95 %) was used to remove these compounds present in the Ti_4N_3 product, since cryolite is soluble in H_2SO_4.[4] This was done by washing the nitride and salt mixture in 4 M H_2SO_4 for 1 h with stirring with a magnetic Teflon coated bar in a ratio of 10 mL 4 M H_2SO_4 : 1 g Ti_4N_3-fluoride mixture. The mixture was then rinsed with deionized (DI) water, centrifuged at 3,500 rpm for 2 min and decanted to separate and dispose of the acid. Rinsing with DI water and centrifuging was repeated until the supernatant liquid in the centrifuge tube had a pH of at least 6. After the last decanting the sediment was then filtered on a polypropylene membrane (3501 Coated PP, Celgard LLC, Charlotte, NC) and will henceforth be referred to as multilayered Ti_4N_3.

To delaminate the multilayered MXene into few-layer and monolayer flakes, the powder was mixed with 40 wt.% tetrabutylammonium hydroxide (TBAOH) (Acros Organics, Morris Plains, NJ; 40% in water) in a ratio of 10 mL TBAOH : 1 g Ti_4N_3 by hand-shaking for 5 min. This procedure has been applied to other MXene systems for this purpose.[5] To separate and remove the TBAOH, the powder was then washed with DI water and centrifuged at 3,500 rpm for 5 min and the supernatant was decanted to remove the residual TBAOH. After that, DI water was added to the residue Ti_4N_3 powder and probe sonicated for 30 min. To separate the smaller delaminated Ti_4N_3 flakes, this suspension was centrifuged at 5,000 rpm for 15 min, and the

supernatant suspension was filtered onto a polypropylene membrane to collect these flakes. Theses flakes are henceforth referred to as delaminated Ti_4N_3.

II. X-ray diffraction

X-ray diffraction (XRD) was carried out on Ti_4N_3 powders using a Rigaku Smartlab (Tokyo, Japan) diffractometer with Cu-Kα radiation (40 KV and 44 mA); step scan 0.02º, 3°–70° 2 theta range, step time of 1 s, 10x10 mm^2 window slit. To identify all of the fluorides formed after the molten salt treatment of Ti_4AlN_3 (Na_3AlF_6, K_2NaAlF_6, K_3AlF_6, AlF_3 and $LiNa_2AlF_6$), a longer scan with a dwell time of 6 s per 0.01º step was applied. To better determine the $Ti_4N_3T_x$ peaks, a long acquisition scan with step size of 0.015º and dwell time of 10 s was performed and shown as the top pattern in Fig. S1. The (0002) and (0004) peaks are more visible compared to the scan with 1 s dwell time (black pattern), which further confirms MXene presence in the final product. Because the small amount of delaminated MXene did not cover the entire glass slide upon which it was scanned, a very broad peak from 20 to 35° is present, which corresponds to the glass. This broad peak is typical of amorphous glass.[6]

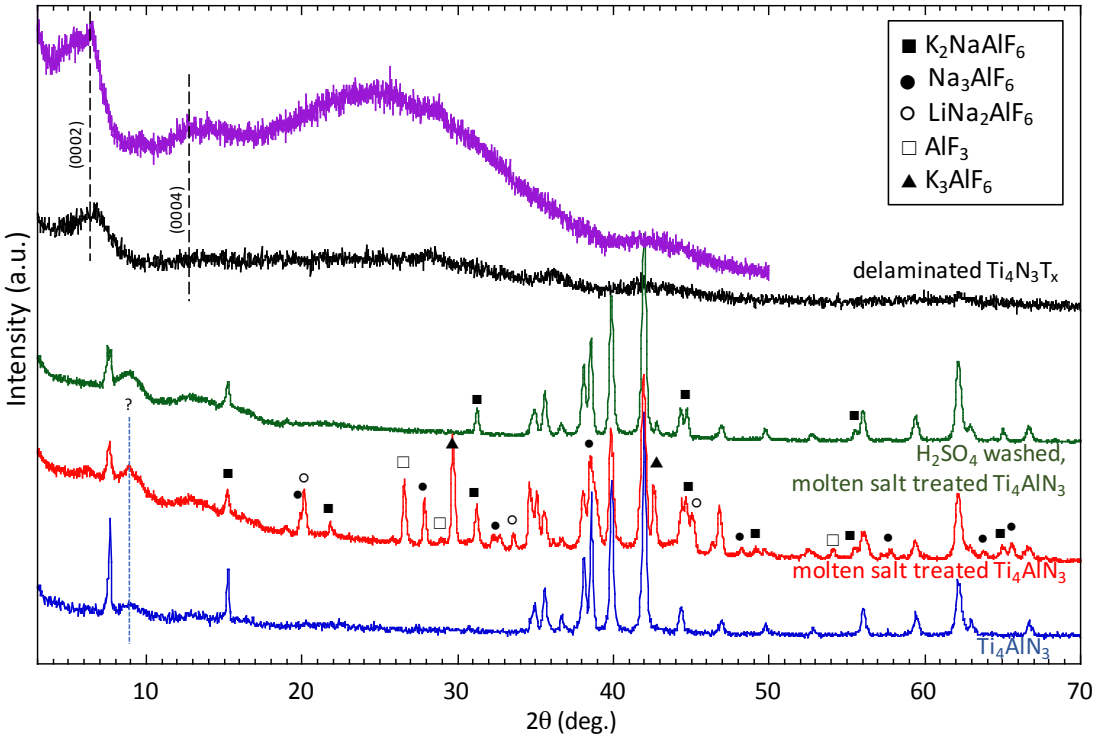

Fig. S1 XRD patterns of Ti_4AlN_3, molten salt treated Ti_4AlN_3, molten salt treated Ti_4AlN_3 after washing in 4 M H_2SO_4, and two patterns of the delaminated $Ti_4N_3T_x$ with different acquisition parameters. After washing Ti_4AlN_3 in H_2SO_4, the peaks attributed to fluorides present in the molten salt treated Ti_4AlN_3 are significantly diminished, signifying that this washing step is effective in removing the fluorides.

III. Scanning Electron Microscopy

To examine the morphology of the nitrides after various steps in the procedure, scanning electron microscopy (SEM) was performed in a Zeiss Supra 50VP (Carl Zeiss SMT AG, Oberkochen, Germany) equipped with an energy-dispersive X-ray spectrometer (EDS) (Oxford EDS, with INCA software). Most EDS scans were obtained at low magnification (100× to 200×) on at least 10 different 0.5 mm by 0.5 mm areas for 60 s on each location. Atomic ratios determined from atomic percentages were calculated by averaging the atomic percentages of all points scanned.

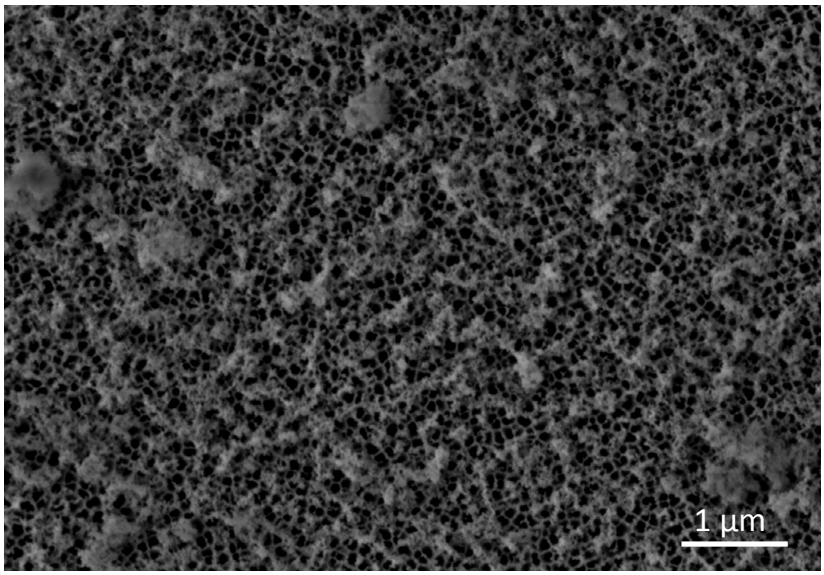

Fig. S2 SEM micrograph of the filtered delaminated $Ti_4N_3T_x$ flake suspension in water, using an alumina filter. The porous structure is the filter. Few-layer and single-layer $Ti_4N_3T_x$ particles on the filter are a few hundred nm in size.

IV. Transmission Electron Microscopy

The JEM-2100 (JEOL, Japan) transmission electron microscope (TEM) was used to analyze MXene flakes with an accelerating voltage of 200 kV. The TEM samples were prepared by dropping two drops of diluted colloidal solution of MXene flakes onto a copper grid and drying in air.

V. Raman Spectroscopy

Raman spectroscopy was performed on a Renishaw inVia (Gloucestershire, UK) microspectrometer by using a 632.8 nm He-Ne laser focused through a 0.7 numerical aperture objective with 63× magnification. The laser spot size in the focal plan was about 1 µm. The back-scattered light from the sample was directed to the CCD detector by a grating with 1200 lines/mm. The setup possesses a spectral resolution of 2 cm^{-1}.

VI. Spin-Polarized Density Functional Theory

The spin-polarized density functional theory (DFT) calculations were performed using the Vienna ab initio Simulation Package (VASP). The projector augmented wave (PAW)

method [7, 8] was used to describe the ion-electron interactions, where valence electrons of Ti, N, F, O, and H are considered with $3d^2 4s^2$, $2s^2 2p^3$, $2s^2 2p^5$, $2s^2 sp^4$, and $1s^1$, respectively. For the exchange-correlation energy, we used the local density approximation (LDA) and the Perdew–Burke–Ernzerhof (PBE) version of generalized gradient approximation (GGA).[9] An energy cutoff of 650 eV was used for the plane wave expansion of the valence electron wave functions. A 12×12×1 Γ-centered Monkhorst−Pack *k*-point mesh was used in the first Brillouin zone to obtain converged results for the $Ti_4N_3T_x$ unit cell during structural relaxation. The convergence criterion was set to 10^{-6} eV/cell in energy and 0.002 eV/Å in force during structural optimization. A vacuum space of 20 Å thick was used to prevent any interactions between the adjacent periodic images of the monolayer. After structural relaxation, a denser *k*-point mesh of 24×24×1 was employed for the calculation of the spin-polarized partial density of states (PDOS).

According to density of states (DOS) at the Fermi level, bare and functionalized Ti_4N_3 MXenes are metallic. These calculations show that bare Ti_4N_3 is magnetic, while the introduction of surface termination groups dramatically lowers the total magnetic moment in the unit cell. Previous work [10] also mentioned this point in both carbide and nitride $Ti_{n+1}X_n$ systems, (X is either C or N) showing a trend of increased total magnetic moment with increasing n for carbides and an almost flat trend for nitrides.

The previously reported work, however, only described the bare MXene without detailed spin-polarized PDOS analysis. In this paper, we clearly show the change in magnetic moment of bare and terminated MXenes from observing the difference between spin-up and spin-down DOS in Fig. 4. The larger the asymmetric character, the larger the magnetic moment. Furthermore, instead of absolute zero magnetic moment, different types of surface terminations reduce the magnetic moment to zero differently. For example, the F-terminated Ti_4N_3 has small total magnetic moment (greater than zero) due to the possible magnetic moment from the surface Ti(3+) atoms. The total magnetic moment of the unit cell will be cancelled out largely by the inner non-magnetic Ti(4+) atoms. Likewise, O and OH groups give a smaller magnetic moment due to the reduced magnetic moment of the surface Ti atoms.

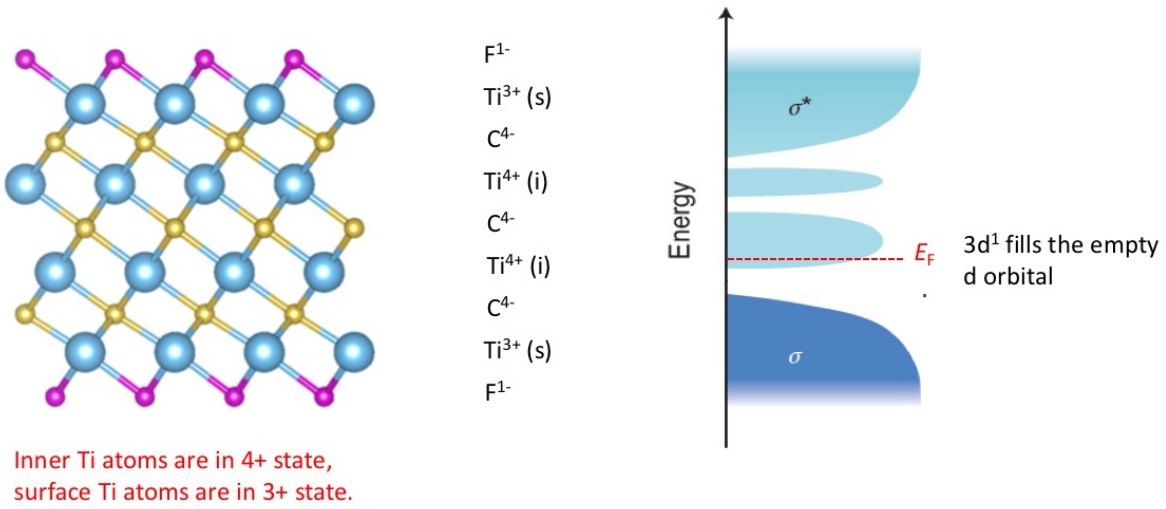

Figure S3 Schematics showing (*left*) the surface and inner Ti atoms, and (*right*) the band structure with *d* electron, which gives a magnetic moment of 1 μB/Ti(s).

References

1 A.T. Procopio, T. El-Raghy, M.W. Barsoum, *Metall. Mater Trans. A*, 2000, **31**, 373-378.
2 J. A. Lane, *Fluid Fuel Reactors*, Addison-Wesley Publishing Co., Inc, Reading, MA, 1958.
3 M. Naguib, V. Presser, D. Tallman, J. Lu, L. Hultman, Y. Gogotsi and M. W. Barsoum, *Journal of the American Ceramic Society*, 2011, **94**, 4556-4561.
4 D. R. Lide, *CRC Handbook of Chemistry and Physics, 83rd Edition*, Taylor & Francis, 2002.
5 M. Naguib, R. R. Unocic, B. L. Armstrong and J. Nanda, *Dalton Trans*, 2015, **44**, 9353-9358.
6 M. Stoica, G. N. B. Maurício de Macedo and C. Rüssel, *Opt. Mater. Express*, 2014, **4**, 1574-1585.
7 P. E. Blöchl, *Physical Review B*, 1994, **50**, 17953-17979.
8 G. Kresse and J. Furthmüller, *Physical Review B*, 1996, **54**, 11169-11186.
9 J. P. Perdew, K. Burke and M. Ernzerhof, *Physical Review Letters*, 1996, **77**, 3865-3868.
10 Y. Xie and P. R. C. Kent, *Physical Review B*, 2013, **87**, 235441.